# Potential limitations in the use of KillerRed for fluorescence microscopy

**Marcus Nordgren[*], Bo Wang[*], Oksana Apanasets[*], Chantal Brees[*], Paul P. Van Veldhoven[*], and Marc Fransen[*]**

[*] Laboratory of Lipid Biochemistry and Protein Interactions, Department of Molecular Cell Biology, Katholieke Universiteit Leuven, Leuven, Belgium

**Correspondence to:** Dr. Marc Fransen, Department of Molecular Cell Biology, Faculty of Medicine, Katholieke Universiteit Leuven, Herestraat 49 box 601, 3000 Leuven, Belgium. Phone: +32(0)16330114; fax: 32(0)16330642; e-mail: marc.fransen@med.kuleuven.be

**Running Head**: Spectral properties of KillerRed

**Keywords**: fluorescent proteins, image analysis, spectral bleed-through, co-localization, LC3, peroxisomes

**Summary**

KillerRed, a bright red fluorescent protein, is a genetically-encoded photosensitizer which generates radicals and hydrogen peroxide upon green light illumination. The protein is a potentially powerful tool for selective light-induced protein inactivation and cell killing, and can also be used to study downstream effects of locally increased levels of reactive oxygen species (ROS). The initial aim of this study was to investigate whether or not KillerRed-mediated ROS production inside peroxisomes could trigger the sequestration of these organelles into autophagosomes. Green fluorescent protein (GFP)-tagged microtubule-associated protein 1 light chain 3 (LC3) was used as autophagosome marker. We observed that KillerRed also emits weak green fluorescence upon excitation at 480 nm, and this may lead to erroneous data interpretation in conditions where green fluorophores are used. We discuss this potential pitfall of KillerRed for biological imaging and formulate recommendations to avoid misinterpretation of the data.

## Introduction

Fluorescence imaging has become a powerful tool to study complex and dynamic processes in biological systems. The portfolio of fluorescent compounds that find wide use in intracellular imaging is rapidly expanding and includes tracker dyes, nanoparticles, and genetically-encoded reporter proteins (Terasaki & Jaffe, 2004; Chudakov *et al.*, 2010; Hinner & Johnsson, 2010; Swanson *et al.*, 2011). The green fluorescent protein (GFP) from the jellyfish *Aequorea victoria* is one of the most widely used fluorescent probes for the labelling of individual proteins or cell compartments for live cell fluorescence microscopy, and the number of GFP variants and GFP-like proteins with distinct spectral characteristics and various maturation rates is rapidly growing (Terasaki & Jaffe, 2004). Nowadays, these proteins are widely used to (i) monitor promoter activity and gene expression, (ii) visualize particular cell types in tissues, organs, and even whole animals, (iii) study protein-protein interactions, (iv) track protein movement, (v) image $Ca^{2+}$, pH, and ROS, and (vi) generate ROS in a spatially and temporally controlled manner (Chudakov *et al.*, 2010; Swanson *et al.*, 2011).

We recently investigated the usefulness of targeted variants of KillerRed (KR) and roGFP2 to locally increase and measure ROS levels in different subcellular compartments in mammalian cells (Ivashchenko *et al.*, 2011). RoGFP2 is a redox-sensitive variant of the enhanced GFP (EGFP) which contains engineered cysteine residues on adjacent surface-exposed β-strands that form a disulfide bond under oxidizing conditions (Hanson *et al.*, 2004). As oxidation of the dithiol pair causes reciprocal changes in emission intensity when excited at ~400 and ~490 nm, the ratio of roGFP2 emissions (at ~510 nm) can provide a non-destructive read-out of the redox environment of the fluorophore (Hanson *et al.*, 2004; Meyer & Dick, 2010). KR is a red fluorescent genetically-encoded photosensitizer that produces

radicals and hydrogen peroxide upon green light illumination (Carpentier *et al.*, 2009; Vegh *et al.*, 2011). The protein has excitation and emission maxima at 585 nm and 610 nm, respectively, and ROS production is accompanied by profound photobleaching (Bulina *et al.*, 2006).

Until now, KR has been used for light-induced cell killing, chromophore-assisted light inactivation (CALI), and manipulation of complex cellular and developmental processes by regulated generation of ROS (Del Bene *et al.*, 2010; Lukyanov *et al.*, 2010; Serebrovskaya *et al.*, 2011). The initial aim of this study was to investigate whether or not this photosensitizer can also be used to selectively damage peroxisomes in mammalian cells and target these organelles for autophagic sequestration. The availability of such an assay may facilitate future studies on the identification of specific signals and markers that target non-functional peroxisomes for autophagic degradation. However, we unexpectedly found that the intrinsic spectral properties of KR complicated the interpretations of the results. As we expect KR to find broad application in live-cell fluorescence imaging, we believe some caution is warranted, especially in case the subcellular localization of green fluorescent reporters will be assayed or quantitative measurements in the green emission channel are necessary.

## Materials and Methods

*Plasmids and DNA manipulation*

The plasmids encoding cytosolic KR (c-KR), peroxisomal KR (p-KR), peroxisomal roGFP2 (p-roGFP2), and GFP-LC3 have been described elsewhere (Kabeya *et al.*, 2000; Ivashchenko *et al.*, 2011). The mCherry DNA template PG27188 (DNA 2.0, Menlo Park, CA) and the mammalian expression vector pEGFP-N1 (Clontech, Mountain View, CA) were commercially obtained. Oligonucleotides were synthesized by Integrated DNA Technologies (Leuven, Belgium). PCR reactions were carried out by employing *Pfx* DNA polymerase (Invitrogen, Merelbeke, Belgium). Restriction enzymes were purchased from TaKaRa (Lonza, Verviers, Belgium). The *Escherichia coli* strain *Top10F'* (Invitrogen) was used for all DNA manipulations. The construct coding for peroxisomal mCherry (p-Ch) (pMF1218) was generated by amplifying the mCherry cDNA fragment by PCR [template: PG27188; forward primer: 5'-gcactgaccgcgcggtgc-3'; reverse primer: 5'-ggcggggcggccgcttacagtttagatttgtacagttcatccgcactgaccgcgcggtgc-3'] and cloning the *Bam* HI/*Not* I-digested PCR-product into the *Bam* HI/*Not* I-restricted backbone fragment of pEGFP-N1. All plasmids were verified by DNA sequencing (LGC Genomics, Berlin, Germany).

*Antibodies*

The rabbit polyclonal sera against EGFP, HsPex13p and HsPex14p have been described elsewhere (Amery *et al*. 2000; Fransen *et al*. 2001). The rabbit polyclonal antibody against LAMP2 (Sigma-Aldrich, Bornem, Belgium) and the goat anti-rabbit IgGs conjugated to Alexa Fluor 350 (Invitrogen) or alkaline phosphatase (Sigma-Aldrich) were commercially obtained.

*Cell culture, transfections, and (immuno)fluorescence microscopy*

The m5-7;GFP-LC3 mouse embryonic fibroblast (MEF) cell line, in which GFP-LC3 is stably expressed and the expression of the autophagy-related gene 5 *(ATG5)* can be regulated by doxycycline administration, and the SV40 large T-antigen immortalized MEFs have been described elsewhere (Hosokawa *et al.*, 2006; Ivashchenko *et al.*, 2011). Cells were cultured at 37°C in a humidified 5% $CO_2$ incubator in minimum essential medium Eagle alpha (MEMα; BioWhittaker) (Lonza) supplemented with 10% (v/v) heat-inactivated South-American fetal calf serum (Invitrogen), 2 mM Glutamax (Invitrogen), and Mycozap (Lonza). m5-7;GFP-LC3 MEFs were cultivated in the presence of 350 µg/ml G418 (Sigma-Aldrich). Cells were transfected by employing the Neon Transfection System (Invitrogen; 1350 V, 30 ms pulse width, 1 pulse) and kept in the dark as much as possible. Cells grown on glass coverslips were fixed and processed for immunofluorescence microscopy as described (Huybrechts *et al.*, 2009). Cells for live-cell imaging were seeded and imaged in FD-35 Fluorodish cell culture dishes (World Precision Instruments, Hertfordshire, England). Fluorescence was evaluated on a motorized inverted IX-81 microscope, controlled by Cell-M software and equipped with (i) a temperature, humidity, and $CO_2$-controlled incubation chamber, (ii) a 100x Super Apochromat oil immersion objective, (iii) the band-pass (BP) excitation filters BP360-370, BP470-495, BP545-580, and D405/20x; (iv) the barrier (BA) filters BA420-460, BA510-550, and BA610IF, (v) dichromatic mirrors with cut-offs at 400, 425, 505, and 600 nm, and (vi) a CCD-FV2T digital B/W camera (Olympus, Aartselaar, Belgium). The camera exposure time was set to 100 and 20 ms to acquire images of peroxisomal roGFP2 (p-roGFP2) at 400 and 480 nm excitation wavelengths, respectively. To generate KillerRed-mediated ROS, the cells were irradiated with green light (100x oil objective, 545-580nm, 1300 µW/cm$^2$) for the indicated time frames. The Olympus image analysis and particle detection software were used for quantitative image analysis.

*Cell fractionation and immunoblotting*

Fractionations of m5-7;GFP-LC3 cells were performed as described (Fransen *et al.*, 2004). Protein extracts were prepared by standard techniques, separated by SDS-PAGE, and analyzed by immunoblotting.

*Statistical analysis*

Statistics were performed on the VassarStats statistical computation website (http://faculty.vassar.edu/lowry//VassarStats.html). One-way analysis of variance was used to determine the differences among independent groups of numerical values, and individual differences were further explored with a Student's t-test. The significance level was chosen to be $p<0.05$.

*Spectral analysis*

The spectral analysis data of the *E. coli*-expressed $(His)_6$-KR were kindly provided by Evrogen JSC (Moscow, Russia). The recombinant protein was purified by using immobilized metal ion affinity chromatography. The ratio between the absorbances at 585 nm and 280 nm was greater than 2.0. Emission spectra were recorded with a Varian Cary Eclipse fluorescence spectrophotometer (excitation and emission slits 5 nm).

## Results

### Expression of peroxisomal KR in m5-7;GFP-LC3 cells: a fluorescence microscopic analysis

As superfluous and non-functional peroxisomes are proposed to be removed by autophagy (Iwata *et al.*, 2006; Kim *et al.*, 2008; Hara-Kuge & Fujiki, 2008; Huybrechts *et al*., 2009), we intended to investigate the cellular fate of photodamaged peroxisomes in mouse embryonic fibroblasts (MEFs) stably expressing GFP-LC3, a widely used marker of autophagosomes in mammalian cells (Hosokawa *et al.*, 2006). Therefore, we transfected these cells with a construct coding for p-KR, a peroxisomal variant of KR (Ivashchenko *et al.*, 2011), and analyzed the co-localization of GFP-LC3 puncta with Pex14p, a peroxisomal marker protein, under different experimental conditions. We surprisingly found that GFP-LC3 and Pex14p displayed a weak but clear co-localization even in the absence of photoirradation (Fig. 1A). No such co-localization could be observed when p-mCherry (p-Ch), another peroxisomally located red fluorescent protein, was expressed in these cells (Fig. 1B) or when p-KR and EGFP were transiently co-expressed in wild-type MEFs (Fig. 1C). Interestingly, expression of p-KR in GFP-LC3 cells also resulted in a small but significant decrease in peroxisome density (Fig. S1A). However, as many of these cells contain peroxisomal aggregates (Fig. S1B), it is not clear whether or not this reduction in peroxisome number can be attributed to the clustering effect (see below). Nevertheless, taken together with our finding that expression of p-KR slightly increases the intraperoxisomal redox status in wild-type MEFs (Fig. S1C), these data suggest that p-KR has a noxious effect on peroxisomes and may target these organelles for autophagic degradation.

**Expression of peroxisomal KR in m5-7;GFP-LC3 cells: a subcellular fractionation analysis**

To confirm that GFP-LC3 is indeed recruited to peroxisomes upon expression of p-KR, we fractionated the postnuclear supernatant of m5-7;GFP-LC3 cells expressing cytosolic or peroxisomal KR by ultracentrifugation using a discontinuous Nycodenz density gradient (Fransen *et al.*, 2004). To our surprise, we couldn't observe a p-KR-dependent banding of GFP-LC3 in peroxisome-enriched fractions (Fig. S2A). This finding suggests that p-KR expression by itself does not target peroxisomes for autophagic degradation.

**KillerRed displays a weak green emission peak upon excitation at 480 nm**

To find an explanation for the apparently conflicting fluorescence microscopy and subcellular fractionation data, we explored two possibilities. First, as (i) the amount of GFP-LC3 associated with peroxisomes may be below the detection limit of our immunoblot analysis, (ii) GFP-LC3 may dissociate from the peroxisomal membrane during the fractionation procedure, or (iii) peroxisomes sequestered in GFP-LC3-positive autophagosomes may acquire a reduced buoyant density which is very similar to lysosomes (Berg *et al.*, 1994), we examined whether or not expression of p-KR resulted in a decreased abundance of peroxisomal proteins in total cell lysates. However, as this was not the case (Fig. S2B), we conclude that the reduced number of peroxisomes in these cells is the result of organelle aggregation, and not organelle degradation. Note that this aggregation phenotype, which can already be observed one day post-transfection (Fig. S3A), is dependent on the expression levels of p-KR (Fig. S3B,C), but not GFP-LC3 (Fig. S3B,D). Second, as the green fluorescence intensities at the peroxisome correlated with the fluorescence intensities of p-KR (Fig. S4), we investigated whether or not p-KR and GFP-LC3 displayed fluorescence cross-

talk in our microscope setting. We first exploited the fact that KR is particularly sensitive to photobleaching (Bulina *et al.*, 2006), and exposed m5-7;GFP-LC3 cells expressing p-KR to green light. As this treatment did not result in a proportional decay of the green and red emission intensities (Figs. 2A and S5A), it can be ruled out that the red fluorescence signals are directly leaking into the green emission channel. Next, we transiently expressed p-KR in wild-type MEFs and quantified the fraction of bleed-through into the green channel. These experiments surprisingly revealed a weak but clear green fluorescence signal at longer exposure times in cells expressing KR at high levels (Fig. 2C). Again, as this result cannot be attributed to leakage of the red signal into the green channel (Figs. 2B and S5B), these data suggest that KR produces a minor green fluorescence signal upon excitation around 480 nm. The correctness of this hypothesis was confirmed by measuring the emission spectra of KR for excitation at 480 nm (Fig. 3A). Additional measurements revealed that the fluorescence intensity of KR's green emission peak at 480 nm excitation is approximately 60 times less than its red emission peak at 570 nm excitation (Fig. 3B).

**Discussion**

The initial aim of this study was to investigate whether or not KR-mediated ROS-production inside peroxisomes could selectively target these organelles for degradation by autophagy. However, during these studies, we discovered that KR produces a minor green fluorescence signal upon excitation around 480 nm, thereby complicating the interpretation of the results. Indeed, as shown in this study, this spectral bleed-through artifact can be easily confused with co-localization of KR and a green fluorophore (*in casu* GFP-LC3) in case the intensities of fluorescence emission are not equally balanced.

As our observations indicate that the apparent co-localization of p-KR and GFP-LC3 in fluorescence microscopy most likely represents a KR-associated artifact, we also faced the problem of how to interpret our observation that the intraperoxisomal redox status slightly increased upon p-KR expression. As (i) oxidation of the dithiol pair of roGFP2 causes an increase in 510 nm emission ratio when excited at 400 and 480 nm (Hanson *et al.*, 2004), and (ii) KR produces a green fluorescence signal upon excitation around 480 but not 400 nm (Fig. 3C), one would expect to see a slight decrease in the emission ratios of p-roGFP2 in case p-KR does not elicit oxidative stress. Nevertheless, as it has also been reported that KR's red chromophore (absorption peak at 585 nm) can be converted into a green chromophore (absorption peak 400 nm) during the early stages of photobleaching and upon treatment with 2-mercaptoethanol (Pletnev *et al.*, 2009), we cannot rigorously rule out the possibility that the small but significant increase in p-roGFP2 oxidation upon p-KR expression is also a KR-associated artifact. However, such an artifact cannot explain why peroxisomes cluster in cells highly overexpressing p-KR. It also remains to be established whether or not KR-containing peroxisomes can be selectively sequestered within autophagosomes upon activation of the photosensitizer. Indeed, due to the unforeseen fact that KR emits green weak fluorescence

upon excitation at 480 nm, it is not possible to address this issue within the current experimental set-up in which a GFP-tagged version of LC3 is used as marker for autophagosomal membranes. However, to address this issue, one can envision other experiments in which – for example – the cells are fixed at well-defined time points after KR-activation and subsequently processed for immunostaining with a primary antibody against an autophagosome marker and a secondary antibody conjugated to a blue fluorophore.

As KR has great potential in a wide range of fluorescence-based applications, we believe it is important for the investigator to be aware of its limitations. Special care should be taken in the design of KR-based studies, in particular when the co-localization of KR and green fluorophores is under investigation or signal intensity measurements are necessary. Potential problems can be circumvented by rigorously controlling the expression levels of KR or by using a threshold value for KR emission. This value, which may vary considerably with different experimental set-up (e.g. filter set, signal integration time needed to collect green image data, …), can be determined by taking fluorescence images of single labeled samples. Alternatively, one can make use of software algorithms for spectral unmixing. In conclusion, the results of this study shed more light on the spectral properties of KR and demonstrate that some caution is warranted in interpreting KR-associated results when the photosensitizer is used in combination with green fluorophores.

**Acknowledgements**

We thank Dr. N. Mizushima (Tokyo Medical and Dental University, Japan) for the m5-7;GFP-LC3 MEF cell line, Dr. M. Pavlenko (Evrogen JSC, Russia) for the emission spectra of KR, and Dr. T. Yoshimori (Osaka University, Japan) for the plasmid encoding GFP-LC3. This work is supported by grants from the 'Fonds voor Wetenschappelijk Onderzoek-Vlaanderen (Onderzoeksproject G.0754.09)' and the 'Bijzonder Onderzoeksfonds van de K.U.Leuven (OT/09/045)'. B. W. is supported by a fellowship of the Chinese Research Council.

**References**


Amery, L., Fransen, M., De Nys, K., Mannaerts, G.P. & Van Veldhoven, P.P. (2000) Mitochondrial and peroxisomal targeting of 2-methylacyl-CoA racemase in humans. *J. Lipid Res.* **41**, 1752-1759.

Berg, T.O., Strømhaug, P.E., Berg, T. & Seglen, P.O. (1994) Separation of lysosomes and autophagosomes by means of glycyl-phenylalanine-naphthylamide, a lysosome-disrupting cathepsin-C substrate. *Eur. J. Biochem.* **221**, 595-602.

Bulina, M.E., Lukyanov, K.A., Britanova, O.V., Onichtchouk, D., Lukyanov, S. & Chudakov, D.M. (2006) Chromophore-assisted light inactivation (CALI) using the phototoxic fluorescent protein KillerRed. *Nat. Protoc.* **1**, 947-953.

Carlsson, S.R., Roth, J., Piller, F. & Fukuda, M. (1988) Isolation and characterization of human lysosomal membrane glycoproteins, h-lamp-1 and h-lamp-2. Major sialoglycoproteins carrying polylactosaminoglycan. *J. Biol. Chem.* **263**, 18911-18919.

Carpentier, P., Violot, S., Blanchoin, L. & Bourgeois, D. (2009) Structural basis for the phototoxicity of the fluorescent protein KillerRed. *FEBS Lett.* **583**, 2839-2842.

Chudakov, D.M., Matz, M.V., Lukyanov, S. & Lukyanov, K.A. (2010) Fluorescent proteins and their applications in imaging living cells and tissues. *Physiol. Rev.* **90**, 1103-1163.

Del Bene, F., Wyart, C., Robles, E., Tran, A., Looger, L., Scott, E.K., Isacoff, E.Y. & Baier, H. (2010) Filtering of visual information in the tectum by an identified neural circuit. *Science* **330**, 669-673.

Fransen, M., Terlecky, S.R. & Subramani, S (1998). Identification of a human PTS1 receptor docking protein directly required for peroxisomal protein import. *Proc. Natl. Acad. Sci. USA* **95**, 8087-8092.

Fransen, M., Vastiau, I., Brees, C., Brys, V., Mannaerts, G.P. & Van Veldhoven, P.P. (2004) Potential role for Pex19p in assembly of PTS-receptor docking complexes. *J. Biol. Chem.* **279**, 12615-12624.

Fransen, M., Wylin, T., Brees, C., Mannaerts, G.P.& Van Veldhoven, P.P. (2001) Human Pex19p binds peroxisomal integral membrane proteins at regions distinct from their sorting sequences. Mol. Cell. Biol. **21**, 4413-4424.

Hanson, G.T., Aggeler, R., Oglesbee, D., Cannon, M., Capaldi, R.A., Tsien, R.Y. & Remington, S.J. (2004) Investigating mitochondrial redox potential with redox-sensitive green fluorescent protein indicators. *J. Biol. Chem.* **279**, 3044-13053.

Hara-Kuge, S. & Fujiki, Y. (2008) The peroxin Pex14p is involved in LC3-dependent degradation of mammalian peroxisomes. *Exp. Cell Res.* **314**, 3531-3541.

Hinner MJ & Johnsson K. (2010) How to obtain labeled proteins and what to do with them. *Curr. Opin. Biotechnol.* **21**, 766-776.

Hosokawa, N., Hara, Y. & Mizushima, N. (2006) Generation of cell lines with tetracycline-regulated autophagy and a role for autophagy in controlling cell size. *FEBS Lett.* **580**, 2623-2629.

Huybrechts, S.J., Van Veldhoven, P.P., Brees, C., Mannaerts, G.P., Los, G.V. & Fransen, M. (2009) Peroxisome dynamics in cultured mammalian cells. *Traffic* **10**, 1722-1733.

Ivashchenko, O., Van Veldhoven, P.P., Brees, C., Ho, Y.S., Terlecky, S.R. & Fransen, M. (2011) Intraperoxisomal redox balance in mammalian cells: oxidative stress and interorganellar crosstalk. *Mol. Biol. Cell* **22**, 1440-1451.

Iwata, J., Ezaki, J., Komatsu, M., Yokota, S., Ueno, T., Tanida, I., Chiba, T., Tanaka, K. & Kominami, E. (2006) Excess peroxisomes are degraded by autophagic machinery in mammals. *J. Biol. Chem.* **281**, 4035-4041.

Kabeya, Y., Mizushima, N., Ueno, T., Yamamoto, A., Kirisako, T., Noda, T., Kominami, E., Ohsumi, Y. & Yoshimori, T. (2000) LC3, a mammalian homologue of yeast Apg8p, is localized in autophagosome membranes after processing. *EMBO J.* **19**, 5720-5728.

Kim, P.K., Hailey, D.W., Mullen, R.T. & Lippincott-Schwartz, J. (2008) Ubiquitin signals autophagic degradation of cytosolic proteins and peroxisomes. *Proc. Natl. Acad. Sci. USA* **105**, 20567-20574.

Lukyanov, K.A., Serebrovskaya, E.O., Lukyanov, S. & Chudakov, D.M. (2010) Fluorescent proteins as light-inducible photochemical partners. *Photochem. Photobiol. Sci.* **9**, 1301-1306.

Meyer, A.J. & Dick, T.P. (2010) Fluorescent protein-based redox probes. *Antioxid. Redox Signal.* **13**, 621-650.

Pletnev, S., Gurskaya, N.G., Pletneva, N.V., Lukyanov, K.A., Chudakov, D.M., Martynov, V.I., Popov, V.O., Kovalchuk, M.V., Wlodawer, A., Dauter, Z. & Pletnev, V. (2009) Structural basis for phototoxicity of the genetically encoded photosensitizer KillerRed. *J. Biol. Chem.* **284**, 32028-32039.

Serebrovskaya, E.O., Gorodnicheva, T.V., Ermakova, G.V., Solovieva, E.A., Sharonov, G.V., Zagaynova, E.V., Chudakov, D.M., Lukyanov, S., Zaraisky, A.G. & Lukyanov, K.A. (2011) Light-induced blockage of cell division with a chromatin-targeted phototoxic fluorescent protein. *Biochem. J.* **435**, 65-71.

Swanson, S., Choi, W.G., Chanoca, A. & Gilroy, S. (2011) *In vivo* imaging of Ca(2+), pH, and reactive oxygen species using fluorescent probes in plants. *Annu. Rev. Plant Biol.* **62**, 273-297.

Terasaki, M. & Jaffe, L.A. (2004) Labeling of cell membranes and compartments for live cell fluorescence microscopy. *Methods Cell Biol.* **74**, 469-489.

Vegh, R.B., Solntsev, K.M., Kuimova, M.K., Cho, S., Liang, Y., Loo, B.L., Tolbert, L.M. & Bommarius, A.S. (2011) Reactive oxygen species in photochemistry of the red fluorescent protein "Killer Red". *Chem. Commun.* **47**, 4887-4889.

## Figure Legends

**Fig. 1. Peroxisomal KR and GFP-LC3 display overlapping fluorescence patterns in m5-7;GFP-LC3 cells.** (A, B) m5-7;GFP-LC3 (m5-7) and (C) control (wt) MEFs were transfected with plasmids encoding (A) peroxisomal KR (p-KR), (B) peroxisomal mCherry (p-Ch) or (C) EGFP and p-KR. Three days later, the cells were fixed and processed for immunostaining with an anti-Pex14p (14) antibody, followed by a secondary antibody conjugated to Alexa Fluor 350. Representative fluorescence micrographs are shown. The exposure times (in ms) are indicated between parentheses. Pex14p and GFP-LC3 were respectively used as a marker for peroxisomes and autophagosomes. Arrowheads indicate selected Pex14p-positive puncta displaying a weak but clear co-localization with GFP-LC3. Bars: 10 μm.

**Fig. 2. Spectral leakage of p-KR.** m5-7;GFP-LC3 (m5-7) and control (wt) MEFs were transfected with a plasmid coding for peroxisomal KR (p-KR). Three days later, the cells were processed for live-cell imaging. (A, B) The cells were exposed to sequential 1-s pulses of green light every 20 s, and images were taken at the indicated time points. (C) Fluorescent micrographs were taken without any other treatment. The relative fluorescence intensities (RFI) emitted in the red and green channels were measured and plotted. Note that (i) the values shown in (A) and (B) are normalized (RFI at $T_0$ = 100%), and (ii) as m5-7 cells express GFP-LC3, a predominantly cytosolic protein, the green emission intensities in the cytosol (C green) are shown in addition to the green (PO green) and red (PO red) emission intensities associated with peroxisomes. Representative results from one of three experiments are shown.

**Fig. 3. Fluorescence emission spectra of KR at 400, 480, and 570 nm excitation.** The fluorescence emission spectra of KR at 400, 480, and 570 nm excitation are indicated in blue, green, and red, respectively. The spectra are normalized using the maximum emission for (A, C) 480 nm excitation, and (B) 570 nm excitation. The areas shaded in gray represent the filter wavelengths of the green (BA510-550) and red (BA610IF) barrier filters.

**Supplementary Figure Legends**

**Fig. S1. Effect of p-KR expression on peroxisomal density, morphology, and redox state.** (A, B) m5-7;GFP-LC3 (m5-7) MEFs were transfected with a plasmid encoding peroxisomal mCherry (p-Ch), peroxisomal KR (p-KR), or cytosolic KR (c-KR). Three days later, the cells were processed for immunostaining with an anti-Pex14p (14) antibody (for more details, see legend to Fig. 1). (A) Quantification of the number of peroxisomes (PO) per cell section ($n > 40$ sections per condition). (B) Fluorescence image of cells transfected with the plasmid encoding p-KR. The insets show magnifications of the marked area of a transfected and a non-transfected cell. The exposure times (in ms) are indicated between parentheses. Bar: 10 μm. (C) Control (wt) MEFs were transfected with a plasmid encoding peroxisomal roGFP2 (p-roGFP2) in the absence (no KR) or presence (p-KR) of a plasmid coding for peroxisomal KR. Three days post-transfection, the cells were processed for live-cell imaging. The relative fluorescence intensities emitted from 400 and 480 nm excitation were used to calculate the 400/480 nm ratiometric response of p-roGFP2. The ratio values represent the mean ± standard deviation ($n > 100$ peroxisomes per condition). Each set of data was statistically compared (* $p < 0.05$).

**Fig. S2. Immunoblot analysis of GFP-LC3 localization and PMP abundance in m5-7;GFP-LC3 cells.** m5-7;GFP-LC3 MEFs were transfected with a plasmid encoding peroxisomal KR (p-KR), cytosolic KR (c-KR), or peroxisomal mCherry (p-Ch). Three days later, whole cell lysates and postnuclear fractions were prepared, and the latter fractions were further subjected to Nycodenz density gradient centrifugation. (A) Equal volumes of the selected gradient fractions (indicated below each set of panels), collected from the bottom of the gradient, and (B) total cell lysates (20 μg of protein) were processed for total protein detection with reversible Ponceau S stain and immunoblotting with Pex14p, EGFP, LAMP2,

or Pex13p antisera. Note that (i) the transfection efficiencies were between 80 and 90% (data not shown), (ii) Pex14p, a peroxisomal marker with a predicted molecular mass of 41 kDa, has an apparent molecular mass of 57 kDa after SDS-PAGE (Fransen *et al.*, 1998), and (iii) the different molecular masses observed for LAMP2, a lysosome-associated membrane protein, are most likely due to the fact that this protein undergoes alternative splicing (leading to at least three different isoforms) and is extensively glycosylated with a variety of N-linked and O-linked oligosaccharides (Carlsson *et al*., 1988). The migration of the relevant molecular mass markers (expressed in kDa) is shown at the left side of each panel.

**Fig. S3. The formation of peroxisome clusters upon p-KR expression is independent of GFP-LC3 expression.** Control (wt) MEFs were not transfected (-) or transfected with a plasmid encoding peroxisomal mCherry (p-Ch), GFP-LC3 (LC3), peroxisomal KR (p-KR), or peroxisomal KR and GFP-LC3 (p-KR LC3). Three days later (unless specified otherwise), the cells were fixed and processed for immunostaining with an antibody specific for Pex14p (14). (A) Peroxisome cluster formation as a function of time (dpt, days post-transfection). (B) Quantification of cells with peroxisome clusters. (C, D) Fluorescence images of cells expressing different levels of (C) p-KR or (D) GFP-LC3. The insets show higher magnifications of the marked areas. N, no expression; L, low expression; H, high expression. Bar: 10 μm.

**Fig. S4. The red and green fluorescence intensities at the peroxisome display a cross-correlation in m5-7;GFP-LC3 cells expressing p-KR.** m5-7;GFP-LC3 (m5-7) MEFs were transiently transfected with a plasmid encoding peroxisomal KR (p-KR). Three days later, the cells were processed for live-cell imaging. A cell containing peroxisomes with an

inhomogeneous fluorescence signal distribution of p-KR is shown. The exposure times (in ms) used to acquire the red (BP545-580, BA610IF) and green (BP470-495, BA510-550) images were 10 and 100 ms, respectively. Bar: 10 μm.

**Fig. S5. Peroxisomal KR produces a minor green fluorescence signal upon excitation around 480 nm.** (A) m5-7;GFP-LC3 (m5-7) and (B) control (wt) MEFs were transfected with a plasmid encoding peroxisomal KR (p-KR). Three days later, the cells were exposed to sequential 1-s pulses of green light every 20 s. Representative fluorescence micrographs taken at the indicated time points are shown. The exposure times (in ms) used to acquire the red (BP545-580, BA610IF) and green (BP470-495, BA510-550) images were 10 and 100 ms, respectively. Bars: 10 μm.

**Fig. 1**

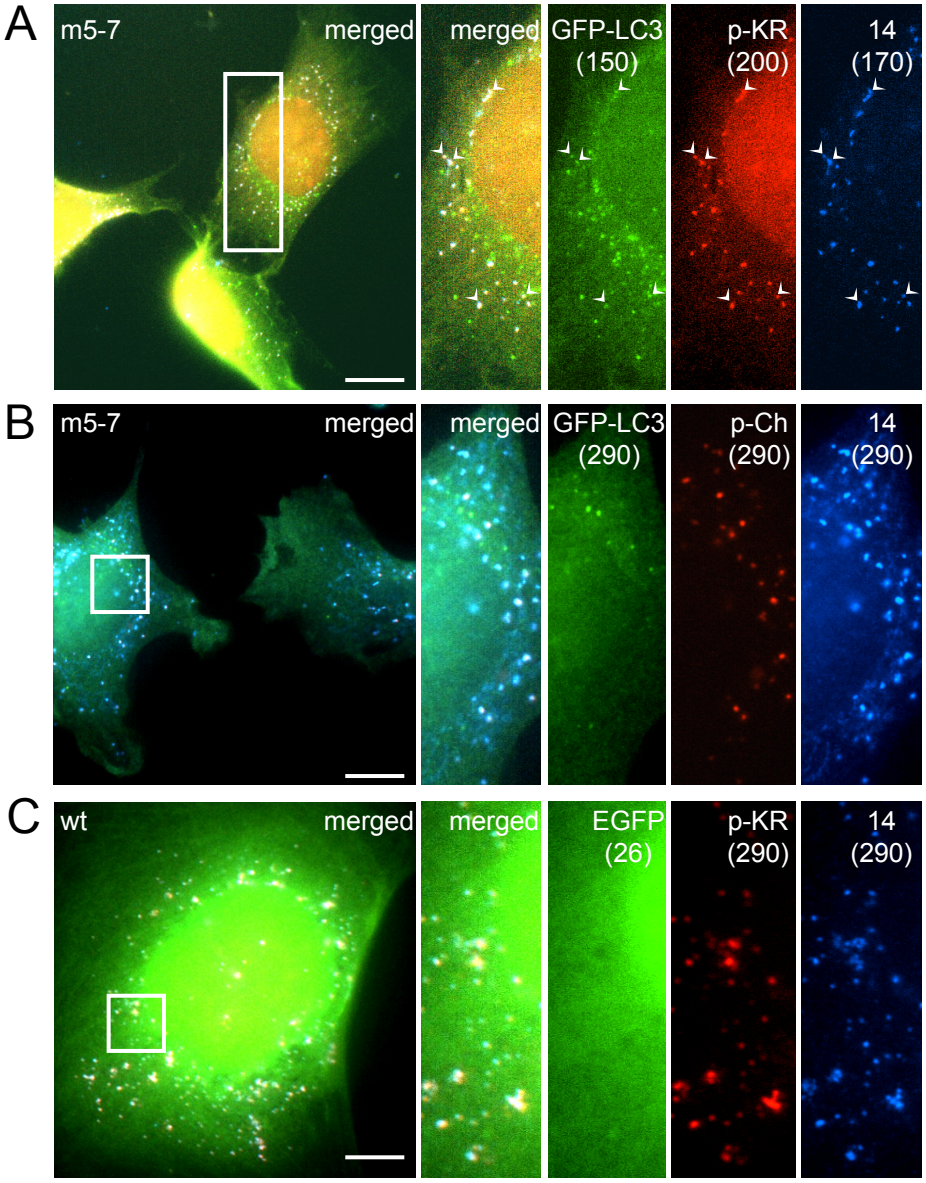
A
m5-7
merged
merged
GFP-LC3
(150)
p-KR
(200)
14
(170)
B
m5-7
merged
merged
GFP-LC3
(290)
p-Ch
(290)
14
(290)
C
wt
merged
merged
EGFP
(26)
p-KR
(290)
14
(290)

**Fig. 2**

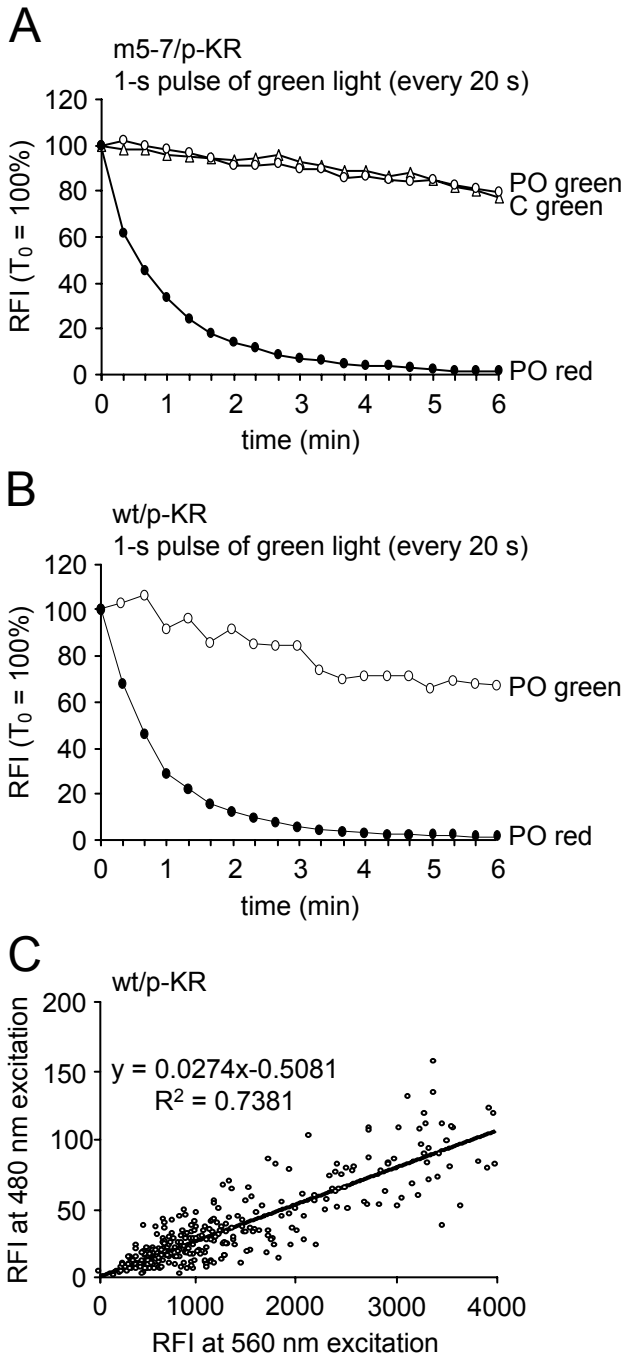
A
m5-7/p-KR
1-s pulse of green light (every 20 s)
RFI ($T_0$ = 100%)
120
100
80
60
40
20
0
0 1 2 3 4 5 6
time (min)
PO green
C green
PO red
B
wt/p-KR
1-s pulse of green light (every 20 s)
RFI ($T_0$ = 100%)
120
100
80
60
40
20
0
0 1 2 3 4 5 6
time (min)
PO green
PO red
C
wt/p-KR
y = 0.0274x-0.5081
$R^2$ = 0.7381
RFI at 480 nm excitation
200
150
100
50
0
0 1000 2000 3000 4000
RFI at 560 nm excitation

**Fig. 3**

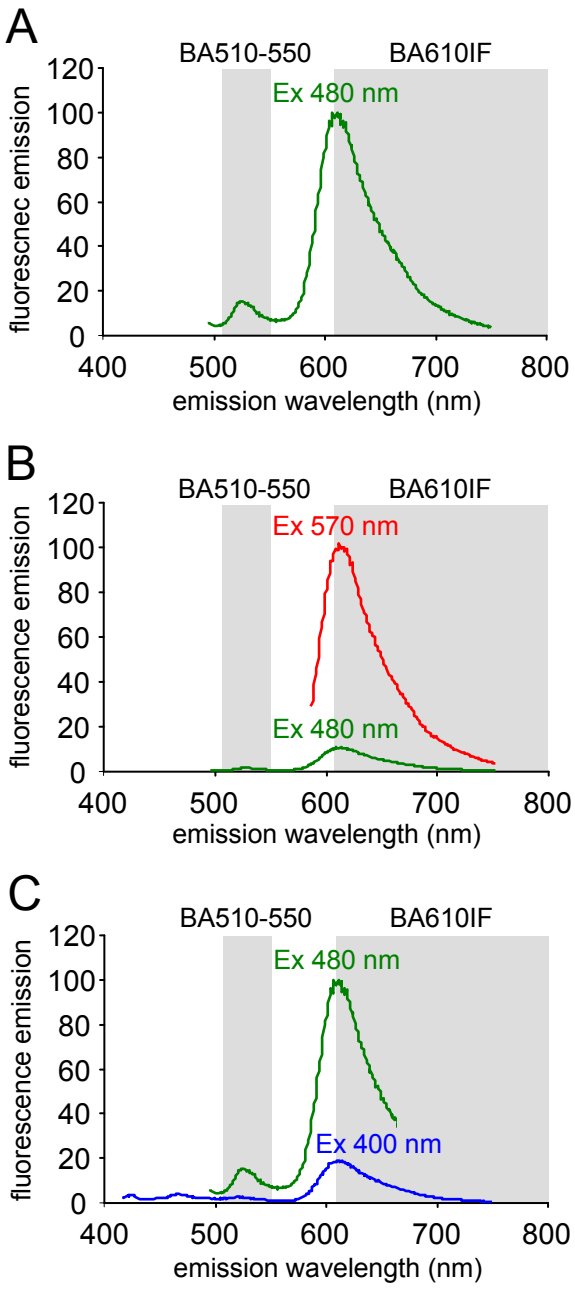
A
BA510-550
BA610IF
Ex 480 nm
fluorescnec emission
120
100
80
60
40
20
0
400
500
600
700
800
emission wavelength (nm)
B
BA510-550
BA610IF
Ex 570 nm
Ex 480 nm
fluorescence emission
emission wavelength (nm)
C
BA510-550
BA610IF
Ex 480 nm
Ex 400 nm
fluorescence emission
emission wavelength (nm)

**Fig. S1**

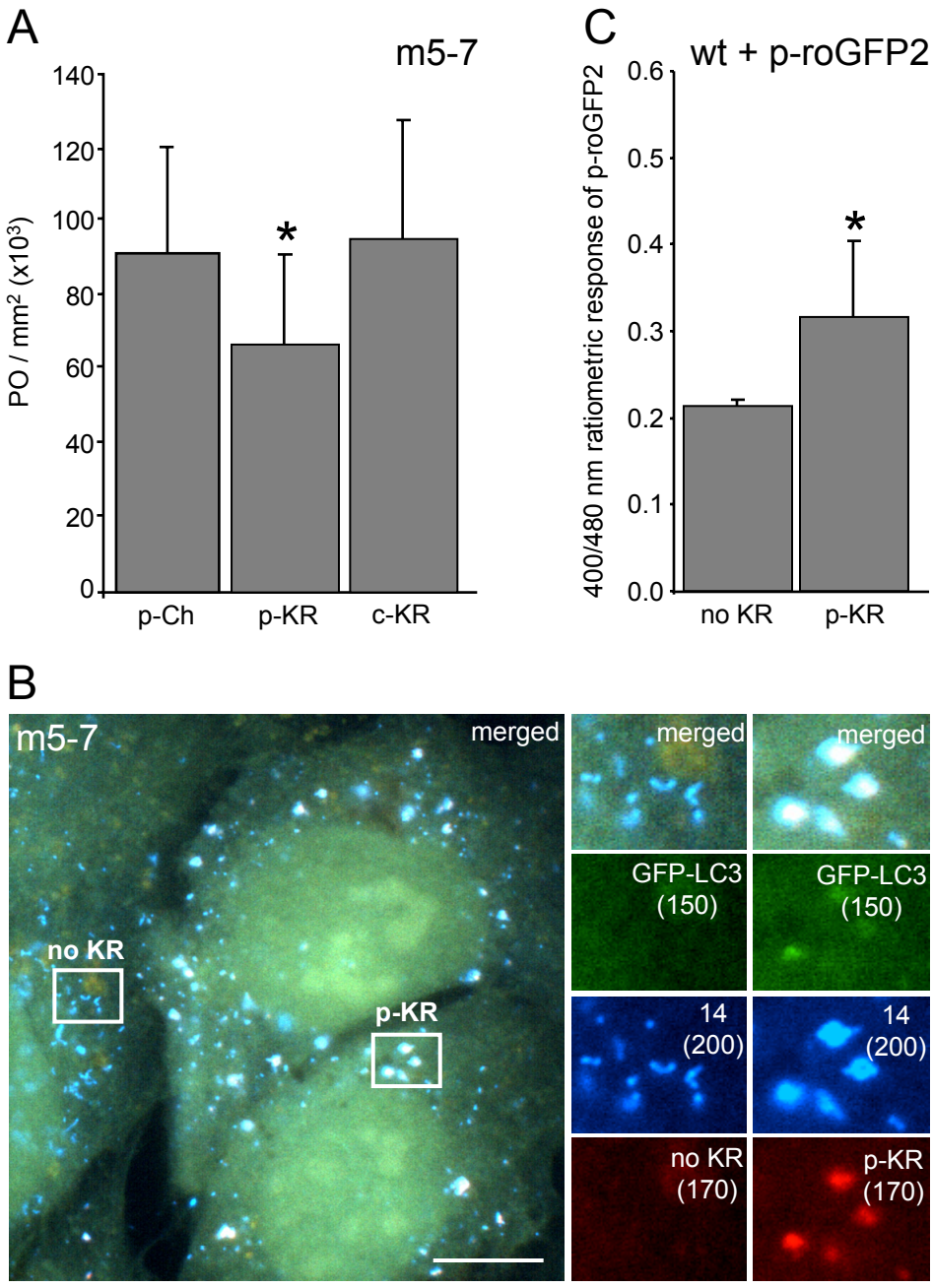
A
m5-7
PO / mm² (x10³)
140
120
100
80
60
40
20
0
p-Ch
p-KR
c-KR
*
C
wt + p-roGFP2
400/480 nm ratiometric response of p-roGFP2
0.6
0.5
0.4
0.3
0.2
0.1
0.0
no KR
p-KR
*
B
m5-7
merged
no KR
p-KR
merged
merged
GFP-LC3
(150)
GFP-LC3
(150)
14
(200)
14
(200)
no KR
(170)
p-KR
(170)

**Fig. S2**

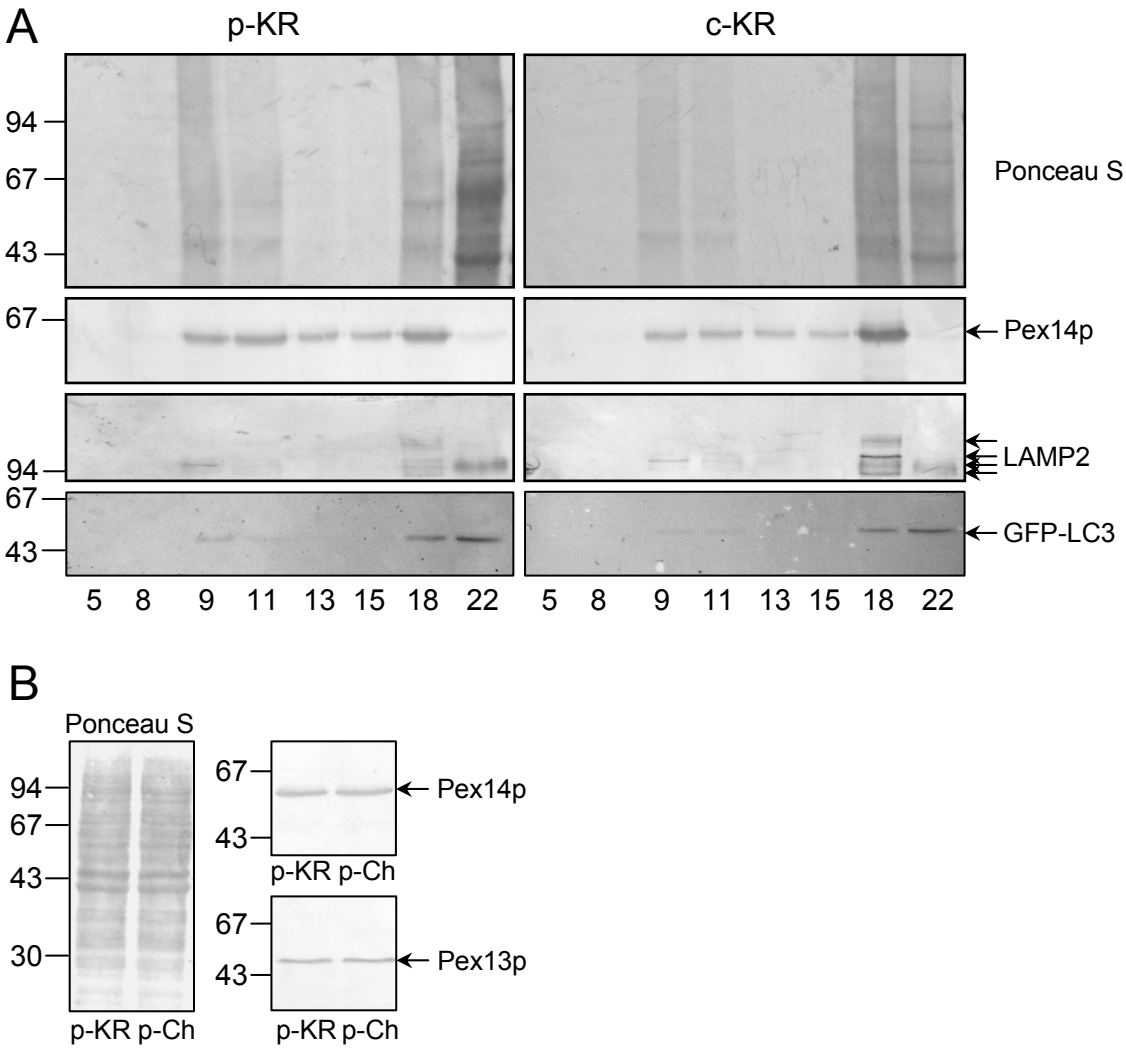
A
p-KR
c-KR
94
67
43
Ponceau S
67
Pex14p
94
67
43
LAMP2
GFP-LC3
5 8 9 11 13 15 18 22
5 8 9 11 13 15 18 22
B
Ponceau S
94
67
43
30
p-KR p-Ch
67
43
Pex14p
p-KR p-Ch
67
43
Pex13p
p-KR p-Ch